IAEA
International Atomic Energy Agency

INDC(NDS)-0561
Distr. G+NM

INDC International Nuclear Data Committee

Missing Level Corrections using Neutron Spacings

G.E. Mitchell

North Carolina State University and
Triangle Universities Nuclear Laboratory

and

J.F. Shriner, Jr.

Tennessee Technological University

November 2009

IAEA Nuclear Data Section, Vienna International Centre, 1400 Vienna, Austria

Selected INDC documents may be downloaded in electronic form from
http://www-nds.iaea.org/indc_sel.html or sent as an e-mail attachment. Requests for hardcopy
or e-mail transmittal should be directed to services@iaeand.iaea.org or to:

Nuclear Data Section
International Atomic Energy Agency
Vienna International Centre
PO Box 100
1400 Vienna
Austria

Produced by the IAEA in Austria
November 2009

INDC(NDS)-0561
Distr. G+NM

Missing Level Corrections using Neutron Spacings

G.E. Mitchell

North Carolina State University and
Triangle Universities Nuclear Laboratory

and

J.F. Shriner, Jr.

Tennessee Technological University

Abstract

Nuclear level densities are very important for a wide variety of pure and applied neutron physics. Most of the relevant information is obtained from neutron resonance data. The key correction to the raw experimental data is for missing levels. All of the standard correction methods assume that the neutron resonances obey the predictions of the Gaussian Orthogonal Ensemble version of Random Matrix Theory (RMT) and utilize comparison with the Porter-Thomas distribution of reduced widths in order to determine the fraction of missing levels. Here we adopt an alternate approach, comparing the neutron data with the predictions of RMT for eigenvalue statistics. Since in RMT the widths and eigenvalues are independent, analysis of the eigenvalues provides an independent analysis of the same data set. We summarize recent work in this area using the nearest neighbour spacing distribution, and we also develop tests that utilize several other eigenvalue statistics to provide additional estimates of the missing fraction of levels. These additional statistics include the key test for long range order – the Dyson-Mehta Δ_3 statistic – as well as the thermodynamic energy (that arises from Dyson's Circular Orthogonal Ensemble), the linear correlation coefficient of adjacent spacings (a measure of short range anti-correlation), and a statistic related to the Q statistic defined by Dyson and Mehta in the early 1960s. Developed FORTRAN code is available at *http://www-nds.iaea.org/missing-levels/*. These tests are applied to the *s*-wave neutron resonances in n + ^{238}U and n + ^{232}Th. The results for ^{238}U are consistent with each other and raise some issues concerning data purity. For the ^{232}Th data, all of the tests are in excellent agreement.

November 2009

TABLE OF CONTENTS

Missing Level Corrections using Neutron Spacings

G. E. Mitchell[1] and J. F. Shriner, Jr.[2]

[1] *North Carolina State University and Triangle Universities Nuclear Laboratory*
[2] *Tennessee Technological University*

I. INTRODUCTION

The Handbook for calculations of nuclear reaction data (RIPL2) [1] treats average neutron resonance parameters as core input for nuclear reaction codes. The key parameters are neutron strength functions, capture widths, and level spacings. Here we focus on level spacings. The emphasis in these statistical approaches is usually on a group of levels with the same quantum numbers – what we shall term a *sequence* of levels. For neutron and proton resonances, the total angular momentum J and parity π are generally the relevant quantum numbers, although other quantities such as isospin are also relevant in some cases.

Ideally one wants a pure and complete set of resonances for the sequence in question – a set of resonances where the quantum numbers assigned for each state are correct (pure) and where all states have been identified (complete). Then the average level spacing is simply $D = \Delta E/(N-1)$, where ΔE is the energy range for the given set of resonances and N is the number of resonances. The problem is that one rarely if ever has a perfect set of resonance data: either (1) levels are missed because experimental sensitivity or resolution prevents their detection or else (2) quantum numbers are misassigned, resulting in missing levels from the sequence of data to which they should belong and spurious levels in a different data sequence. We limit the discussion here to s-wave resonant states with spin-zero targets; for such situations, there are no ambiguities in J, and therefore, purity of the sequence is much easier to attain.

Although in principle one could resolve almost all misassignment issues by performing additional experiments (e.g., neutron capture), in practice such an approach is usually considered too expensive (in personnel, accelerator time, etc.) to pursue. There are a variety of tests that are applied to assess the quality of the assignments. For example the difference in penetrabilities for orbital angular momenta $\ell = 0$ and $\ell = 1$ at very low energies is so large that s-wave resonances are normally much stronger than p-wave resonances. One usually formalizes this with a Bayesian analysis [2], but this approach is not always reliable in the gray area between weak s-wave resonances and strong p-wave resonances. Another approach is to compare the number of small spacings with the number expected from the standard Random Matrix prediction; an example of this approach, albeit with proton resonances, is given in [3]. However, this approach provides only an overall estimate of the data quality as regards to misassignments.

In this report we focus on missing level corrections. In Section II we summarize the standard methods for determining the fraction of missing levels and then discuss the motivation for newer methods in Section III. In Section IV we discuss various measures that utilize eigenvalues and then in Section V we consider the effect of missing levels on these measures. We then apply these methods to a few special cases. The final section provides a brief summary.

II. STANDARD METHODS

Essentially all of the methods for determining the fraction of missing levels assume the correctness of the Gaussian Orthogonal Ensemble (GOE) version of Random Matrix Theory (RMT). From early days it was clear that a statistical theory was needed to describe the properties of nuclear resonances. The early developments are given in the compilation by Porter [4]. By the early 1970s sufficient data were obtained (primarily by Rainwater *et al.* – see, e.g., Refs. [5, 6]) to confirm the predictions of RMT. However, due to limited sample size the results were not considered definitive until Bohigas *et al.* [7] combined the best available neutron resonance data (largely by Rainwater's group) and the best available proton resonance data (by the TUNL group [8]) together into the so-called Nuclear Data Ensemble. The data agreed very well with the RMT predictions. The status of RMT was covered in a classic review by Brody *et al.* [9]. A more recent comprehensive review was given by Guhr *et al.* [10], while the status of RMT in nuclear physics is discussed in a

recent review by Weidenmüller and Mitchell [11]. The methods for determining the completeness of the sequence can be divided into three groups – those that utilize (A) the nuclear widths, (B) the spacings, and (C) a combination of the widths and spacings. Throughout this report, we denote the fraction of true levels observed by the variable f. We also utilize the fraction of missing levels, denoted by f_m and related to f via $f_m = 1 - f$.

Before performing a quantitative analysis, it is often convenient to perform a qualitative evaluation of the data set. One simple and useful tool is the number plot – $N(E)$ vs. energy, where $N(E)$ is the number of levels with $E_i \leq E$. The number plot should have a constant slope if the sequence is pure and complete or if the degree of incompleteness/impurity remains constant throughout the energy range. A decrease in slope at higher energies is usually indicative of an increase in the fraction of missing levels. Based on this qualitative assessment one can proceed, perhaps by restricting the analysis to a more limited energy range. Another useful plot is the nearest neighbor spacing distribution. Again, visual inspection is often valuable. For example, since the probability of having a value of $x = S/D$ (S is the spacing between adjacent levels of the sequence, and D is the average spacing) greater than three is about 0.1% for the GOE distribution, an excess number of large values of x provide conclusive proof of missing levels. Examples of the application of this approach are given in Ref. [3]. Another useful plot is the cumulative sum of the resonance widths. The existence of non-statistical effects is often evident as an anomalous bump in an otherwise smooth curve. With these qualitative tests one has a estimate of the overall data quality.

A. Width analysis correction methods

The oldest and most standard methods use the width distribution. For the GOE, the matrix elements (the reduced width amplitudes) follow a Gaussian distribution. Since one measures the widths (not the amplitudes), the result for the width distribution is a chi-squared of one degree of freedom [12]. In nuclear physics this is often labeled the Porter-Thomas distribution :

$$P_{PT}(\gamma^2) = \frac{1}{\sqrt{2\pi\gamma^2 \left\langle\gamma^2\right\rangle}} \exp\left(-\frac{\gamma^2}{2\left\langle\gamma^2\right\rangle}\right), \tag{1}$$

where γ^2 is the reduced width and $\left\langle\gamma^2\right\rangle$ the average reduced width. This result is normalized so that

$$\int_0^\infty P(\gamma^2)\, d\gamma^2 = 1 \tag{2}$$

In terms of the dimensionless variable

$$y \equiv \frac{\gamma^2}{\left\langle\gamma^2\right\rangle}, \tag{3}$$

the Porter-Thomas distribution becomes

$$P_{PT}(y) = \frac{1}{\sqrt{2\pi y}} \exp\left(-\frac{y}{2}\right). \tag{4}$$

Suppose that one has a sequence of N_{obs} levels with the same assigned J^π in the energy range $[E_{min}, E_{max}]$. The goal is to utilize these data to determine the level density in this energy range for this particular J^π value. We assume that the true width distribution is Porter-Thomas. The simplest method to correct for missing levels is the one that has normally been adopted: all of the resonances with reduced widths smaller than the smallest observed reduced width, γ^2_{min}, are assumed to be missed, and all resonances with reduced widths larger than γ^2_{min} are assumed to be observed. In terms of the variable y, it is convenient to define a cut-off parameter y_0 such that all values below $y = y_0$ are missed and all values above y_0 are observed. An initial estimate for y_0 is

$$y_0 = \frac{\gamma^2_{min}}{\left\langle\gamma^2\right\rangle_{obs}}. \tag{5}$$

where $\langle\gamma^2\rangle_{obs}$ is the observed average reduced width:

$$\langle\gamma^2\rangle_{obs} = \frac{1}{N_{obs}} \sum_{i=1}^{N_{obs}} \gamma_i^2. \tag{6}$$

In practice, $\langle\gamma^2\rangle_{obs}$ will be larger than the true value of $\langle\gamma^2\rangle$ due to the effects of missing levels with the smallest widths. To correct for missing levels, the goal is to determine for a given sequence of levels the fraction f of the levels observed. The procedure is widely discussed in the literature (see, e.g., Ref [13]).

Another method of correcting for missing levels [14] that uses the width distribution is based on calculating moments of the observed widths and comparing them to expected values for a Porter-Thomas distribution. This particular method focuses on and is primarily sensitive to larger widths. Although this method has some attractive features, it has some flaws in common with the standard methods. We address these issues in Section III.

B. Spacing analysis methods

Experimental spacing distributions are almost universally used to test if a set of eigenvalues agree with GOE predictions. The most common of these distributions is the nearest-neighbor spacing distribution (NNSD), although sometimes other measures are used. However, with very few exceptions, only recently have methods been developed that utilize the spacings to determine the fraction of missing levels. In Section III we discuss the need for such methods and in Section IV we derive and/or discuss a number of missing level correction methods that use various different characteristics of the spacings.

C. Combined width and spacing methods

Fröhner provides a general survey of the various methods as of a generation ago [13]. However, it is not clear how widely these more sophisticated methods have been applied. A very interesting work that considered both the widths and spacings is by Porodzinskij *et al.* [15]. They emphasize that levels are missed due to both an experimental threshold of observability and to finite resolution effects and attempt to deal with both effects. However, it is not clear how extensively these methods have been applied. They certainly have had little or no impact on the evaluation methods used by experimentalists.

III. MOTIVATION FOR NEWER METHODS

The importance of reliable values for the neutron strength functions (and therefore of the average widths and level spacings) is universally accepted. Their importance to pure and applied physics is crucial in efforts ranging from astrophysical calculations to advanced fuel cycle issues. However, there are still significant disagreements, not only between different experimental measurements, but between different analyses of the same data sets. A striking, recent example is the disagreement between results of the RIPL2 compilation [1] and those of Mughabghab [16]. Therefore there is a need for both a critical evaluation of the existing methods (for missing level determination) and for new methods.

At least in the general literature the method that is used overwhelmingly is that described in the previous section. Assume the Porter-Thomas distribution, determine the cutoff parameter (from the weakest level and the average width), assume that all levels above the weakest level are observed, and integrate the PT distribution from the cutoff value of the dimensionless width parameter y to infinity. The validity of the assumption that all levels are observed above the cutoff value depends largely on the experimental resolution. It is somewhat less of a problem for spin-zero targets because of the level repulsion between states of the same symmetry. Of course the correct separation of s and p states is crucial: even for spin-zero targets, the misassignment of an $\ell = 1$ state as an $\ell = 0$ state can skew the estimate of f dramatically. If the assumption that

all levels below some threshold are observed is true except for a single state, that single state will effectively determine the value of f obtained from this analysis. If the width of that single state is significantly smaller than the cutoff (as might well occur if a p-wave resonance were misassigned as an s-wave resonance), the analysis will produce a value of f that is much too large. Of course methods that focus on the larger widths avoid this particular issue.

An equally important limitation of this standard method is one that has not been emphasized – its sensitivity to non-statistical effects. This is easiest to demonstrate for proton resonances, where isobaric analog states are a common non-statistical effect and have been very well studied. In medium and heavy nuclei, isobaric analog resonances are usually much stronger than typical resonances in the sequence. These strong resonances make the average reduced width larger and the cut-off parameter smaller; this of course also produces an erroneously large value of f when the standard width analysis techniques are applied. Therefore, such non-statistical states should be removed from a data set before a statistical analysis is performed. For isobaric analog states this removal often can be performed with a great deal of confidence. For neutron resonances, there are many cases where non-statistical effects are present, but it is not obvious how to correct for them (see, e.g., Koehler *et al.* [17]). In practice, detailed analysis is often required even to determine whether the observed phenomenon is a true non-statistical effect or simply a statistical fluctuation. Theoretical analysis is normally not helpful in this regard, since it is not possible to predict with sufficient accuracy the presence of three-particle two-hole or other similar states. The best that one can do is to examine the experimental cumulative widths carefully to search for evidence of such effects. The standard method may or not be flawed in any particular case.

In these circumstances an alternative method that is not subject to these problems seems desirable. The key to the solution is the fact that in RMT the eigenvalues and eigenfunctions are independent. Therefore the widths and spacings are independent. In the next section we describe a number of methods that use the spacings in order to determine the missing level fraction. Of particular importance is the fact that the spacings are unaffected by the non-statistical effects that can plague analysis based on the width distribution [18]. Even if methods based on both general approaches agree, which they often do, having an additional measure of f should lead to increased confidence in the results as well as reduced uncertainties. In fact, independent of the issue of the possible impact of non-statistical effects on the width correction method, the advantages of additional independent evaluations of the same data set would seem to be of significant value.

As discussed briefly in Sect. II C, one can consider combining the width and spacing analyses. Although this at first glance is tempting, we believe that, since the width and spacing methods have quite different strengths and weaknesses and are independent of one another, they should be considered separately.

IV. EIGENVALUE MEASURES

There are a number of tests that are used to determine whether a given spectrum agrees with the predictions of Random Matrix Theory; some of these are well known and frequently applied, while others are rather obscure. In principle almost any of these measures could be used to determine the missing level fraction. In this section, we describe a number of these measures for possible application to the missing level problem. We first discuss the nearest-neighbor spacing distribution for which the entire probability density distribution is utilized to characterize a set of eigenvalues. Then we discuss four different statistics that represent the eigenvalues by a single number. We close this section with a discussion of "spectral averaging" as we apply it to the four statistics that return a single number.

In what follows, we use a common notation to the extent possible. N denotes the number of levels in the spectrum, and f indicates the fraction of levels observed (i.e., $f = 1$ corresponds to no missing levels). In all cases, the analysis assumes that the level density is constant over the energy range $[E_{min}, E_{max}]$ in question; if the energy range is sufficiently large that this is not true, an unfolding procedure such as that described in Ref. [3] must be applied. Our discussion below refers to energy levels E_i after any necessary unfolding has been performed.

A. Nearest-neighbor spacing distribution (NNSD)

The most common eigenvalue test is the nearest-neighbor spacing distribution, the so-called Wigner surmise. One of the advantages of this statistic is that the effect of missing levels on the probability density function can be analytically determined.

The nearest-neighbor spacings (the spacings between two adjacent levels) of a perfect GOE sequence are well described by the Wigner distribution

$$P_{GOE}(x) = \frac{\pi}{2} x \mathrm{e}^{-\pi x^2/4}. \tag{7}$$

Here $x \equiv S/D$, where S is a spacing between adjacent levels and D is the average spacing. Since in practice the level sequence is almost always incomplete, we need the distribution that describes the spacing distribution of an imperfect sequence. The key difference between the spacing and width analyses is that the spacings are missed at random. However, an additional difference is that missing a level means that two nearest-neighbor spacings which should be observed are not, while one second-nearest-neighbor spacing (corresponding to one intervening level) is included in the data set although it should not be. Thus, the probability density function for an sequence with missing levels must reflect the inadvertent presence of these higher order spacings. Also important is the fact that the experimental value of the average spacing D_{obs} differs from the true value D according to $D = fD_{obs}$. It proves convenient to derive results in terms of D_{obs}, so we define a variable $z \equiv S_{obs}/D_{obs}$ for that purpose, where S_{obs} is a spacing between adjacent *observed* levels, and D_{obs} is the *observed* average spacing. The variables x and z are related by $z = fx$.

The nearest-neighbor spacing distribution (NNSD) can be written as

$$P(z) = \sum_{k=0}^{\infty} a_k \lambda P(k; \lambda z), \tag{8}$$

where the functions $P(k, x)$ represent the probability density functions for the distributions of spacings when there are k intermediate levels between the two determining the spacings. (Therefore, $P(0, x)$ will be the nearest-neighbor spacing distribution – the Wigner distribution – given in Eq. 7.) The parameters a_k give the relative contributions of these k-th nearest-neighbor spacing distributions $P(k; \lambda z)$, and λ is a parameter that characterizes the incompleteness of the sequence. This form for the probability density function for the spacing distribution of an imperfect sequence was first introduced as an ansatz in 1981 by Watson, Bilpuch, and Mitchell [19]. The results have since been formally derived (using different methods) in Refs. [20] and [21]:

$$P(z) = \sum_{k=0}^{\infty} (1-f)^k P(k; z/f); \tag{9}$$

converting to the variable x yields

$$P(x) = \sum_{k=0}^{\infty} f(1-f)^k P(k; x). \tag{10}$$

For $f = 1$ this reduces to the Wigner distribution $P(0; x)$ as it should. For f near 1 the series converges rapidly – one intervening level is much more likely to be missed than are two, etc. – but the convergence is slower when a larger fraction of the levels is missed.

Obviously, to perform calculations one needs expressions for the $P(k; x)$ functions which give the probability that there are k levels contained in a spacing x between two levels. A closely related set of functions are the $E(k; x)$, which give the probability that a randomly chosen interval of length x contains exactly k levels. Numerical values for $E(k; x)$ and recursive analytical formulae for $E(k; x)$ are given in [22]. The $P(k; x)$ functions and the $E(k; x)$ functions are related by a recursion formula

$$P(k; x) = \sum_{j=0}^{k} (k - j + 1) \frac{d^2}{dx^2} E(j; x). \tag{11}$$

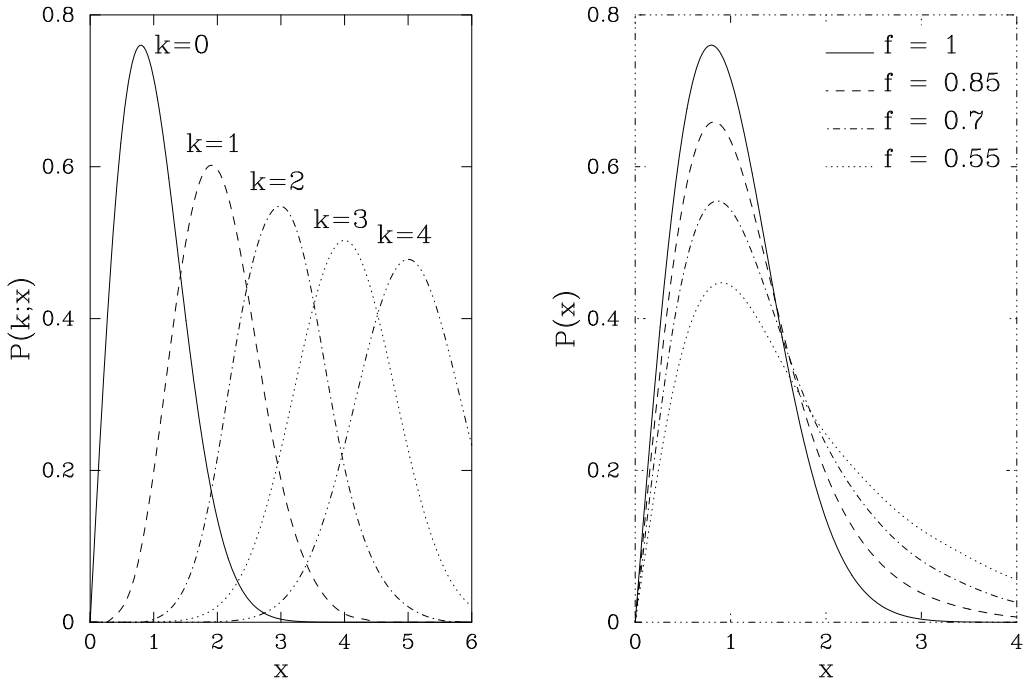

FIG. 1: The left half of the figure shows approximations (as discussed in the text) for the functions $P(k;x)$ for $k \leq 4$ and $x \leq 6$. The right half of the figure shows $P(x)$ for several values of f.

Thus in principle the spacing distribution $P(k;x)$ for any order of k can be found in terms of functions $E(k;x)$.

We have adopted a simpler approach by determining the functions $P(1;x)$ and $P(2;x)$ numerically [20]. An ensemble of 3000 Gaussian Orthogonal matrices of dimension 110 was generated and the $k = 1$ and $k = 2$ nearest-neighbor spacing histograms were calculated for a total of 330,000 levels. $P(k,1)$ can be approximated by a polynomial interpolation and $P(k,2)$ by a rational function interpolation [23]. For $k \geq 3$, $P(k,x)$ is well approximated by a Gaussian distribution centered at $k+1$. (In fact even the $k = 1$ and $k = 2$ functions are reasonably well approximated by Gaussians.) The variance of these distributions was shown by French *et al.* [24] to be approximately

$$\sigma_k^2 = \frac{1}{\pi} \ln\left(2\pi[k+1] + \gamma + 1\right) - \frac{5}{12}, \tag{12}$$

where $\gamma \approx 0.577$ is Euler's constant. The $P(k;x)$ functions for $k \leq 4$ are shown in Fig. 1, along with $P(x)$ from Eq. (10) for several values of f.

B. Δ_3 statistic

While the NNSD approach to the missing level problem has received the most attention in recent years, the earliest approaches generally focused on characterizing the eigenvalue spectrum by a single statistic. Several potential statistics were introduced in the early works by Dyson and Mehta [25–29], and the so-called Δ_3 statistic [28] has been utilized regularly since that time. Δ_3 is determined by comparing the best fit straight line to the number plot (also known as the "staircase function") $N(E)$ for the spectrum eigenvalues. The best fit for this continuous function is defined as the line that minimizes the integral of the square of the difference between the line and $N(E)$, and Δ_3 is defined in terms of that same difference:

$$\Delta_3 = \min_{A,B} \frac{1}{E_{max} - E_{min}} \int_{E_{min}}^{E_{max}} [N(E) - AE - B]^2 dE. \tag{13}$$

In practice, it is easier to evaluate Δ_3 by utilizing a result from Ref. [30]; define a new set of levels ϵ_i centered on $E = 0$ and lying in the interval $[-L, L]$:

$$\epsilon_i \equiv E_i - (E_{min} + E_{max})/2, \tag{14}$$

$$L \equiv (E_{max} - E_{min})/2. \tag{15}$$

Then Δ_3 can be evaluated in terms of L and the set of ϵ_i:

$$\Delta_3 = \frac{N^2}{16} - \frac{1}{4L^2}\left[\sum_{i=1}^{N}\epsilon_i\right]^2 + \frac{3N}{8L^2}\left[\sum_{i=1}^{N}\epsilon_i^2\right] + \frac{3}{16L^4}\left[\sum_{i=1}^{N}\epsilon_i^2\right]^2 + \frac{1}{2L}\left[\sum_{i=1}^{N}(N-2i+1)\,\epsilon_i\right]. \tag{16}$$

For GOE statistics, the expected value must be evaluated numerically, but for large N approaches

$$\Delta_3(N) \approx \frac{1}{\pi^2}\left[\ln N - 0.0687\right]. \tag{17}$$

The effect on the average value of Δ_3 due to missing levels has been given by Bohigas and Pato [21]. In terms of the missing fraction f_m, this can be expressed

$$\Delta_3(f_m, N) = f_m\frac{N}{15} + (1-f_m)^2\,\Delta_{3,GOE}\left(\frac{N}{1-f_m}\right). \tag{18}$$

C. Thermodynamic energy U

One aspect of RMT that was introduced over 40 years ago by Dyson [25, 27] is that of the thermodynamics of the ensembles. Quantities such as free energy, internal energy, entropy, and specific heat were studied, and expected values were obtained for each of the standard ensembles (orthogonal, unitary, and symplectic). Although Dyson used the internal energy as a test for missing levels, this test has apparently not been utilized to evaluate experimental data since. In Ref. [31] we investigated the internal energy U as a test both to evaluate spectra and to determine the missing level fraction. In particular, we examined how this statistic behaves as a function of spectrum size and how it is affected by the presence of missing or spurious levels in the spectrum. Here we simply summarize the computational details.

As with Δ_3, the computation is most simply expressed when the energy range in question is centered on $E = 0$. Furthermore, this particular discussion assumes an average spacing of 1 (in appropriate units). Achieving these requires applying two transformations to the values $\{E_i\}$, the first to normalize the average spacing and the second to center the eigenvalues:

$$\mathcal{L} \equiv N/2, \tag{19}$$

$$\varepsilon_i \equiv \frac{2\mathcal{L}-1}{E_N - E_1}E_i, \tag{20}$$

$$\epsilon_i \equiv \varepsilon_i - \left(\varepsilon_1 + \mathcal{L} - \frac{1}{2}\right). \tag{21}$$

The result is most easily expressed by defining a potential energy:

$$V(E) \equiv (\mathcal{L}-E)\left[\frac{1}{2} + \ln\left(\frac{\mathcal{L}-E}{2\mathcal{L}}\right)\right] + (\mathcal{L}+E)\left[\frac{1}{2} + \ln\left(\frac{\mathcal{L}+E}{2\mathcal{L}}\right)\right]. \tag{22}$$

We also must define a so-called "picket fence" spectrum, a spectrum which has equally spaced levels located at energies

$$\xi_i \equiv -\mathcal{L} + i - \frac{1}{2}. \tag{23}$$

The statistic U can then be calculated:

$$U = -\frac{1}{N}\left[\sum_{j>i}\ln\left|\frac{\epsilon_j - \epsilon_i}{j-i}\right| + \sum_i\left[V(\epsilon_i) - V(\xi_i)\right]\right]. \tag{24}$$

The expected value of U for a GOE spectrum is $1 - \frac{1}{2}\gamma - \frac{1}{2}\ln 2 \approx 0.365$. We are unaware of any theoretical discussion of the effects of missing levels on U.

D. $\hat{Q}$ statistic

In the same paper in which Dyson and Mehta defined Δ_3, they set out to design a statistic similar to U but with reduced variance [28]. They chose the label Q for this statistic. Once again, the statistic is defined in terms of energies centered about zero, so we define a renormalized set of energies and a scaling variable L

$$\begin{aligned} \epsilon_i &\equiv E_i - (E_1 + E_N)/2, \\ L &\equiv \begin{cases} (E_N + E_{max})/2 & \text{if} \quad E_{max} - E_n < E_1 - E_{min} \\ (E_{min} + E_1)/2 & \text{otherwise} \end{cases} \end{aligned}$$

The definition also requires a quantity R with the dimensions of energy. R should satisfy the inequality $D < R < L$, where D is the average spacing. Dyson and Mehta then define Q as follows in terms of some initially unspecified function $f(\epsilon_i, \epsilon_j)$:

$$\begin{aligned} Q &\equiv -\sum_{i<j} f(\epsilon_i, \epsilon_j) \ln \left| \frac{\epsilon_i - \epsilon_j}{R} \right| + \sum_{i,j} F(\epsilon_i) U(\epsilon_j) - \frac{1}{2} U_0 \sum_{i,j} F(\epsilon_i) F(\epsilon_j) \\ &+ \frac{1}{2} \left[\sum_i F(\epsilon_i) \right] \ln \left(\frac{2\pi R \sum_i F(\epsilon_i)}{\int F(\epsilon)\, d\epsilon} \right), \end{aligned} \tag{25}$$

$$U(E) \equiv \frac{\int f(\epsilon, \epsilon') \ln \left| \frac{\epsilon - \epsilon'}{R} \right| d\epsilon'}{\int F(\epsilon')\, d\epsilon'}, \tag{26}$$

$$U_0 \equiv \frac{\int \int f(\epsilon, \epsilon') \ln \left| \frac{\epsilon - \epsilon'}{R} \right| d\epsilon\, d\epsilon'}{\left(\int F(\epsilon')\, d\epsilon' \right)^2}, \tag{27}$$

$$F(\epsilon) \equiv f(\epsilon, \epsilon). \tag{28}$$

Only after this development do Dyson and Mehta specify a specific function for $f(\epsilon_i, \epsilon_j)$; one of their concerns in 1963 in choosing a function was computational complexity, which is certainly not an issue today in this regard, but we will utilize the same choice they made:

$$f(x, y) \equiv \begin{cases} 1 & \text{for} \quad |x - y| < R, |x| < L, |y| < L \\ 0 & \text{otherwise.} \end{cases} \tag{29}$$

This choice of f produces great simplifications in several other quantities:

$$\begin{aligned} F(x) &= \begin{cases} 1 & \text{if} \quad |x| < L \\ 0 & \text{otherwise} \end{cases}, \\ U(x) &= \begin{cases} -R/L & \text{if} \quad |x| < L - R, \\ -\frac{1}{2L} \left[R + (L - |x|) \left(1 - \ln \frac{L - |x|}{R} \right) \right] & \text{if} \quad L - R < |x| < L \end{cases}, \\ U_0 &= -\frac{R}{L} + \frac{R^2}{8L^2}. \end{aligned} \tag{30}$$

We still must specify the parameter R, which Dyson and Mehta suggest should be "a few times the mean-level-spacing D" and characterized in terms of a variable $M \equiv R/D$. After tests of several different values, we chose $M = 4$ for our calculations.

The expected value of Q for a GOE spectrum is given in terms of the internal energy U as

$$\langle Q \rangle \approx n \left[U - \frac{1}{\pi^2 M} \right], \tag{31}$$

where $n \equiv 2L/D$ is approximately the number of observed levels. Since $\langle Q \rangle$ scales with n, it proves convenient to define a statistic

$$\hat{Q} \equiv \frac{Q}{n} \tag{32}$$

to facilitate comparing results from different size spectra. The expected value for $\hat{Q}$ with $M = 4$ is thus ≈ 0.340. As with U, we are unaware of any discussion of exactly how Q is affected by missing levels.

E. Linear correlation coefficient ρ

A final statistic is the linear correlation coefficient between adjacent spacings. A spacing is given by

$$S_i = E_{i+1} - E_i. \tag{33}$$

The linear correlation coefficient is then

$$\rho(S_i, S_{i+1}) = \frac{\sum_i \left(S_i - \langle S_i \rangle\right)\left(S_{i+1} - \langle S_{i+1} \rangle\right)}{\left[\sum_i \left(S_i - \langle S_i \rangle\right)^2 \sum_i \left(S_{i+1} - \langle S_{i+1} \rangle\right)^2\right]^{1/2}}. \tag{34}$$

For GOE spectra, adjacent spacings are anti-correlated with an expected value $\rho = -0.27$ [9]. Again, we are unaware of any analysis of how ρ is affected by missing levels.

F. Spectral Averaging

For the statistical measures that produce a single numerical value to represent an entire spectrum, we face the issue of estimating an uncertainty for that value. A useful way to do this is via the "spectral averaging" approach discussed in some detail for Δ_3 by Mulhall *et al.* [32]. The idea is to divide the spectrum into a series of smaller subintervals, calculate the statistic for each of those subintervals, and then use the (unweighted) mean and its standard deviation as the appropriate value and uncertainty characterizing the statistic for that particular spectrum. Following our earlier tests of different size subintervals and their effects on the statistic U [31], we take our subintervals to be of size $N/2$; unlike our earlier work (and following Mulhall *et al.*), we have chosen subintervals such that each one starts one level or one average spacing beyond the previous one. Thus, there are $\approx N/2$ subintervals as well. However, these are not all independent subintervals due to the overlaps; only the first and last ones are completely independent of each other. Thus in determining the uncertainty of the mean value, we calculate the standard deviation for all subintervals but divide it only by $\sqrt{2}$ (due to only two independent values) to yield an estimated uncertainty of the mean.

V. EFFECTS OF MISSING LEVELS

A. Methods

In section IV, a number of different statistical measures were discussed. For each of them, the expected behavior for a GOE spectrum is known; for some of them, the effect of missing levels in the spectrum has also been quantified. However, these numerical results are often asymptotic limits which may only be truly expected for large spectra. Before relying on those results, it is important to study exactly how these measures behave in finite spectra. We have done this via Monte Carlo studies.

We have chosen to study the behavior of each statistical measure for spectra of sizes $N = 20, 50, 100, 200, 500,$ and 1000. This range spans the sizes of spectra that might generally be observed in nuclear physics and which are large enough that a statistical approach might reasonably be considered. For each value of N, we generated 2500 GOE spectra of size $N_m \approx 1.1N$ and identified the central N levels of each spectrum as our raw data. All the measures assume a constant level density, whereas the GOE spectra definitely do not have a constant level density. Therefore it is necessary to unfold the level density. The level density for a GOE spectrum with N_m levels follows the so-called semicircle law:

$$\rho(E) = \begin{cases} \frac{1}{2\pi}\sqrt{4N_m - E^2} & \text{if } -2\sqrt{N_m} \le E \le 2\sqrt{N_m} \\ 0 & \text{otherwise} \end{cases}. \tag{35}$$

The corresponding $N(E)$ function is

$$N(E) \equiv \int_0^E \rho(E')dE' = \frac{1}{4\pi} E\sqrt{4N_m - E^2} + \frac{N_m}{\pi} \sin^{-1}\left[\frac{E}{4N_m}\right]. \tag{36}$$

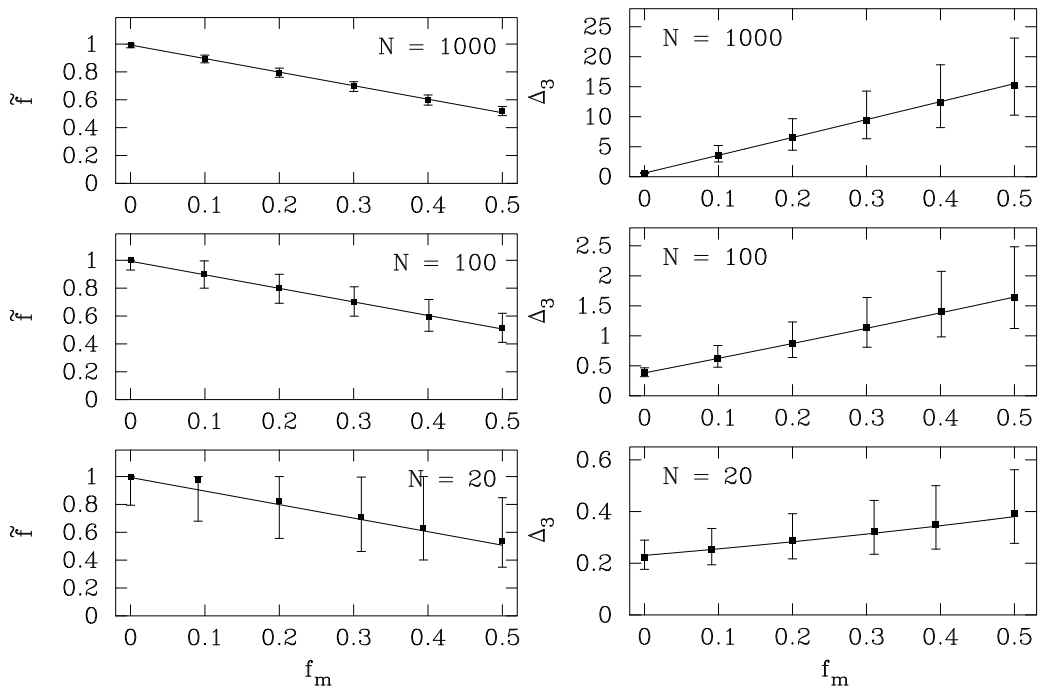

(a) The solid lines represent the best-fit function of $\tilde{f}$ given in Eqn. (38).

(b) The solid lines represent the best-fit function of Δ_3 given in Eqn. (39).

FIG. 2: Median values $\tilde{f}$ as a function of f_m (left) and Δ_3 (right) for the $N = 20$ (lower), $N = 100$ (center), and $N = 1000$ (upper) cases, respectively. Within the uncertainties, there is no dependence on N.

The reason that we take $N_m > N$ is to eliminate any levels whose energies might lie outside the semicircle due to their random nature. For the N central levels of the spectrum, a set of new energy levels which have uniform level density are defined by

$$E'_i = N(E_i), \tag{37}$$

where $N(E)$ is given by Eq. (36). These then serve as the eigenvalues for the various analyses.

To simulate missing levels, we follow a similar procedure but start with a larger spectrum and randomly remove levels from the interior of the spectrum until the desired value of N is achieved. For all these simulations, we find it convenient to express the results in terms of the missing fraction f_m. We have chosen to simulate missing fractions f_m of ≈ 0.1, 0.2, 0.3, 0.4, and 0.5 (in addition to the complete spectra discussed above, which correspond to $f_m = 0$). For each value of N and each value of f_m, 2500 new spectra are generated.

Once the ensemble of spectra is generated for a given choice of N and f_m, we calculate the statistic of interest for each of the 2500 spectra. Each ensemble is then characterized by its median with uncertainties estimated based on the 16th and 84th percentiles of the ensemble. A number of the statistics in question produce asymmetric distributions, and therefore the median value, representing the point at which half of the values should be larger and half smaller, seems more likely to represent what one might obtain from a single experimental spectrum than does the more common mean. Similarly, these empirical estimates of uncertainty also give a range of values that better characterize the expectations for the purposes discussed here. We then utilize standard fitting techniques to determine a function that describes the median behavior as a function of both N and f_m. In most cases, a linear description proves appropriate when either N or f_m is varied by itself. Cross-terms involving both N and f_m are sometimes necessary for a simultaneous description in terms of both variables. The following sections summarize the fits we have identified for the various statistics.

B. NNSD Method

Although the analysis described above of the nearest-neighbor spacing distribution provides a direct estimate of f (we shall call this estimate $\tilde{f}$) and its uncertainty for a single spectrum, we still need to ensure that our extraction of the missing fraction f also reflects the fact that the process of determining f itself introduces some uncertainty because the spectra themselves provide a range of values of f. To do this we have determined an empirical function that describes $\tilde{f}$ as a function of f_m and find that the best fit is linear:

$$\tilde{f}(f_m, N) = a_0 + a_1 f_m, \tag{38}$$

with parameters $a_0 = 0.993 \pm 0.086$ and $a_1 = -0.972 \pm 0.026$. (In reality a complete error matrix resulting from the determination of a_0 and a_1 is utilized to extract the uncertainty of f_m. The complete error matrix is given in the appendix.) The behavior is illustrated in Fig. 2(a).

C. Δ_3 Method

To characterize the behavior Δ_3 as a function of f and N, we start with Eq. (18), recall that our spectral averaging techniques uses subintervals of size $N/2$, and introduce additional coefficients to account for the finite spectral sizes and the use of the median:

$$\Delta_3(f_m, N) = b_0 f_m \frac{N}{30} + b_1 \left(1 - f_m\right)^2 \Delta_{3,GOE}\left(\frac{N}{2\left[1 - f_m\right]}\right). \tag{39}$$

The best fit parameters are $b_0 = 0.920 \pm 0.081$ and $b_1 = 0.978 \pm 0.064$. The behavior of the fitting function is shown in Fig. 2(b).

D. U Method

A linear fit provides an appropriate description of U for variations in either N or f_m alone. This is illustrated in Figure 3(a). The best-fit function is

$$U(f_m, N) = c_0 + (c_1 + c_2 N) f_m, \tag{40}$$

with parameters $c_0 = 0.363 \pm 0.013$, $c_1 = 0.85 \pm 0.14$, and $c_2 = 0.00183 \pm 0.00028$.

E. $\hat{Q}$ Method

$\hat{Q}$ is consistent with being independent of N and linear in f_m as shown in Fig. 3(b). The best-fit function is

$$\hat{Q}(f_m, N) = d_0 + d_1 f_m, \tag{41}$$

with parameters $d_0 = 0.337 \pm 0.011$ and $d_1 = 0.897 \pm 0.052$.

F. ρ Method

As was true with $\hat{Q}$, the linear correlation coefficient ρ is consistent with being independent of N and linear in f_m, as shown in Fig. 3(c). The best-fit function is

$$\rho(f_m, N) = e_0 + e_1 f_m \tag{42}$$

with parameters $e_0 = -0.251 \pm 0.016$ and $e_1 = 0.428 \pm 0.057$.

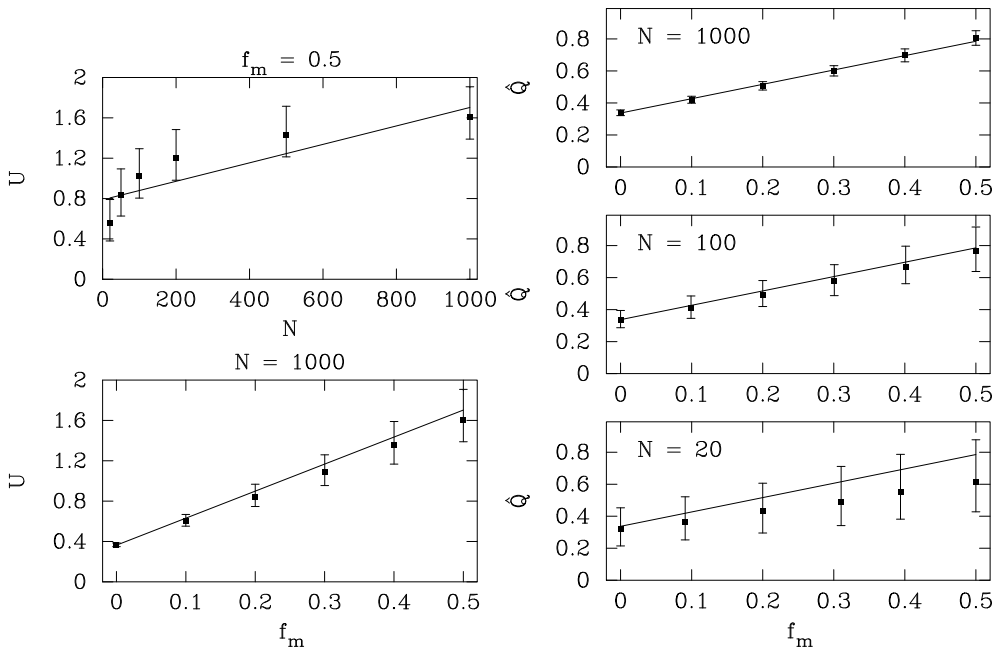

(a) Median values of U as a function of f_m for the $N = 1000$ case (lower), and as a function of N for $f_m = 0.5$ (upper). Error bars are smaller than the points in some cases. The solid lines represent the best-fit function of $U(f_m, N)$ given in Eqn. (40).

(b) Median values of $\hat{Q}$ as a function of f_m for the $N = 20$ (lower), $N = 100$ (center), and $N = 1000$ (upper) cases. Within the uncertainties, there is no dependence on N. The solid lines represent the best-fit function of $\hat{Q}(f_m, N)$ given in Eqn. (41).

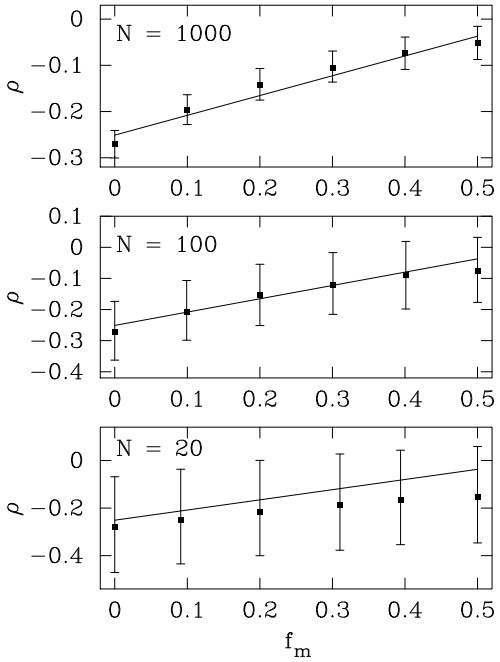

(c) Median values of the linear correlation coefficient ρ as a function of f_m for the $N = 20$, $N = 100$, and $N = 1000$ cases. Within the uncertainties, there is no dependence on N. The solid line represents the best-fit function of $\rho(f_m, N)$ given in Eqn. (42).

FIG. 3: Median values of U (top-left), $\hat{Q}$ (top-right), and linear correlation coefficient ρ (bottom), respectively.

VI. APPLICATIONS

As an application of these methods we examine s-wave resonances in the n + ^{238}U system; our data are from the ENDF compilation [33, 34]. There are 897 such states in the neutron energy range $0 - 20$ keV. These data not only provide a large statistical sample to test the method but also allow one to examine smaller energy ranges and still have sufficient statistics.

Figure 4(a) (see next page) shows the number plot for these states. Of special note is that the slope appears to decrease above $\approx 10 - 12$ keV. This suggests that there may be levels missing at higher energies.

Next, we examine reduced widths for these levels in two different forms. Fig. 4(b) shows the cumulative reduced width as a function of energy, while Fig. 4(c) shows the distribution of reduced widths.

The cumulative sum shows no obvious non-statistical effects. However, the distribution plot shows that the assumption of a sharp cutoff below which all widths are missed and above which all widths are observed is not valid. Therefore, any method that relies on the smallest width to estimate the missing fraction f will not give a reliable estimate for these data.

We turn now to the eigenvalue statistics, beginning with the nearest-neighbor spacing distribution. This is illustrated in Fig. 4(d). The NNSD analysis gives $f = 0.88$, and the distribution corresponding to this value is also shown on Fig. 4(d).

The results for the other four eigenvalue statistics discussed here are shown in Fig. 5. In each case, the value of the statistic is represented by a black horizontal band, while the behavior as a function of f_m is shown by the crossed band. Specific values of f are listed in Table I. Note that for these data, the five different statistics give results for f which are all consistent with each other. We have performed a similar analysis for five subsets of these s-wave resonances, corresponding to 4-keV intervals, and those results are also listed in Table I (the corresponding graphs for the $0 - 4$ keV region are included in Appendix II). The table also provides the weighted average of the five values of f.

TABLE I: Estimates of f for s-wave resonances in the n + ^{238}U system with the different methods. Results for several different energy ranges are listed, along with the value of D obtained for each one.

Energy Range (keV)	Number of Levels	Statistic					Overall Results	
		NNSD	Δ_3	U	$\hat{Q}$	ρ	f	D_0 (eV)
$0 - 20$	897	0.88 ± 0.03	0.80 ± 0.09	0.83 ± 0.07	0.82 ± 0.06	0.81 ± 0.08	0.85 ± 0.02	19.0 ± 0.6
$0 - 4$	187	$1.05^{+0.02}_{-0.03}$	$0.99^{+0.02}_{-0.01}$	1.02 ± 0.02	$1.04^{+0.02}_{-0.03}$	1.08 ± 0.09	1.02 ± 0.01	$21.5^{+0.8}_{-0.9}$
$4 - 8$	183	$0.96^{+0.04}_{-0.06}$	0.97 ± 0.02	0.87 ± 0.05	0.84 ± 0.06	0.85 ± 0.13	$0.95^{+0.01}_{-0.02}$	$20.8^{+0.8}_{-0.9}$
$8 - 12$	186	$0.85^{+0.07}_{-0.08}$	0.82 ± 0.04	0.75 ± 0.09	0.80 ± 0.07	0.91 ± 0.06	0.85 ± 0.03	17.8 ± 0.9
$12 - 16$	169	0.73 ± 0.09	0.74 ± 0.08	0.62 ± 0.09	0.70 ± 0.04	0.53 ± 0.07	0.67 ± 0.03	16.0 ± 0.9
$16 - 20$	172	$0.70^{+0.08}_{-0.10}$	0.49 ± 0.15^a	0.46 ± 0.16^a	0.69 ± 0.08	0.74 ± 0.09	0.67 ± 0.04	$15.6^{+1.1}_{-1.3}$

[a]Values below 0.5 require extrapolation and should be viewed with caution.

Several observations can be drawn from these numbers: **1.** It is notable that the subset results for f are consistent with missing more levels as the energy increases. This agrees qualitatively with our previous assessment of the number plot (Fig. 4(a)). **2.** At large values of f, the different methods are in very good agreement. At smaller values of f, there seems to be more variation among the values obtained by the different method, although the individual values are not in strong disagreement. For the highest energy range, we even find two values of f that lie slightly below the range $[0.5, 1.0]$ over which we established our interpolating functions. **3.** The estimate of D_0 falls as the energy increases. We know from the number plot that there appear to be more missed levels as the energy increases, and the values obtained for f reflect that trend as discussed above, but there is no physical reason to expect D_0 itself to actually be getting smaller. The most likely explanation is that at these higher energies, there are really two issues with the data that these results reflect. It is likely that more levels are missed due to experimental limitations, but it is also likely that some p-waves have been mistakenly assigned as s-waves. The tests we have utilized tend to produce values of f that are too low when spurious levels are included.

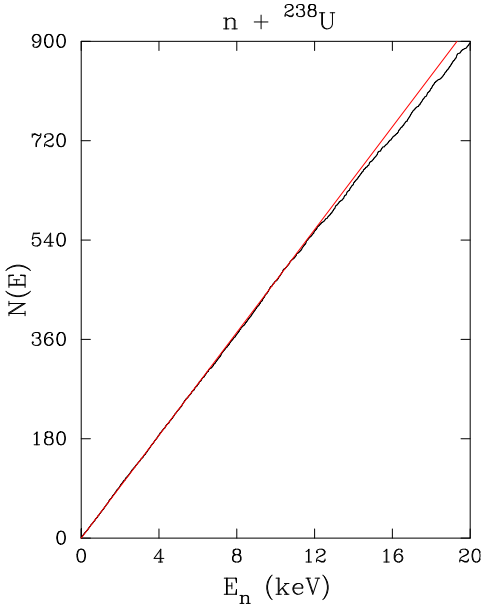

(a) Number plot. The thin red line represents the behavior expected based on the data for $0-4$ keV.

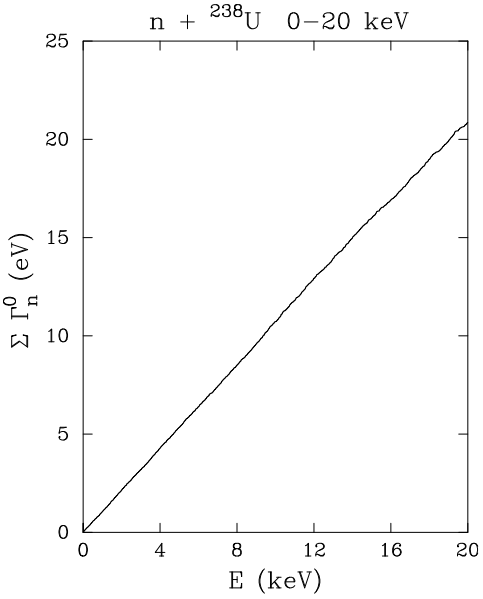

(b) Cumulative sum of reduced widths.

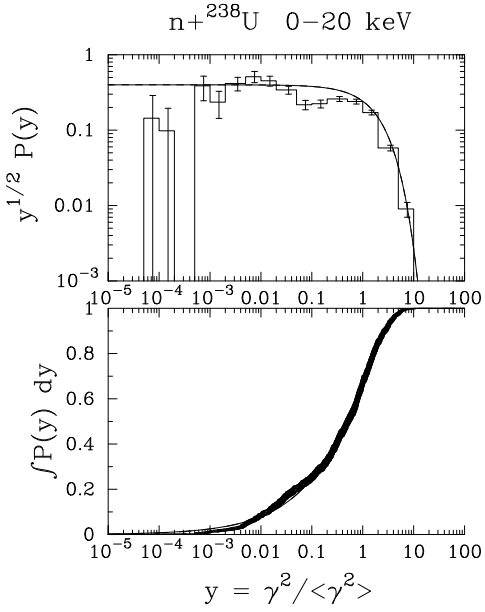

(c) Distribution of reduced widths. The upper part of the figure shows a histogram, while the lower portion shows the probability distribution function. Note the "hole" in the data for values of $y \approx 2-5\times10^{-4}$.

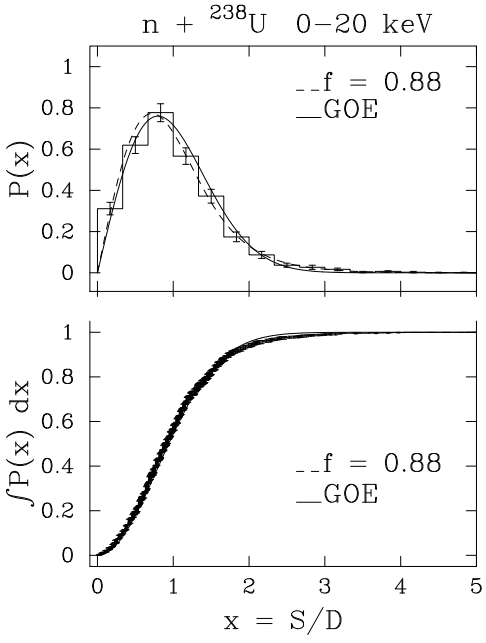

(d) Nearest-neighbor spacing distribution for s-wave resonances in the n + ^{238}U reaction. The probability density function (upper) and the probability distribution function (lower) are shown.

FIG. 4: Analysis of s-wave resonances in the n + ^{238}U reaction in the neutron energy range $0-20$ keV.

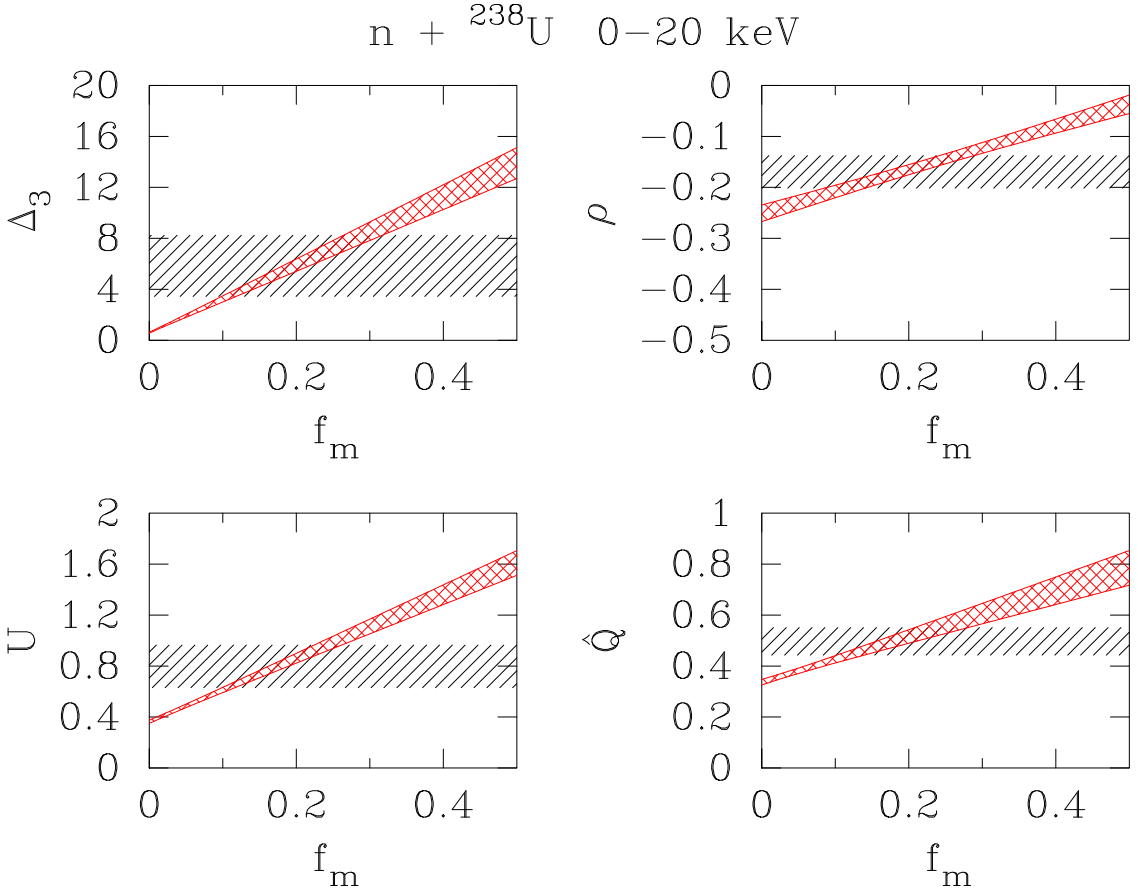

FIG. 5: Analysis of Δ_3, U, $\hat{Q}$ and ρ for the s-wave resonances in the n + ^{238}U reaction. The black dashed horizontal bands in each case represent the value of that statistic (± one standard deviation), and the crossed bands show the expected behavior (again, ± one standard deviation) as a function of f_m for $N = 897$.

As discussed in Sect. I, the average level spacing is a key parameter. Over the entire 20 keV range, the observed average level spacing for 897 s-wave resonances is $D_{obs} = 22.3$ eV. The relative statistical uncertainty in this value is given by Lynn [35] as $\sqrt{0.27/N}$. When combined with the overall value $f = 0.85 \pm 0.02$, the best estimate for this energy range is $D_0 = 19.0 \pm 0.6$ eV. On the other hand, using only the first 4 keV of resonances, an energy range where the data appear to be of higher quality, yields a value $D_0 = 21.5^{+0.8}_{-0.9}$ eV. These values can be compared to the value $D_0 = 20.3 \pm 0.6$ eV of Capote *et al.* [36] and the value $D_0 = 20.26 \pm 0.72$ eV cited in the most recent compilation by Mughabghab [16].

We have also analyzed results for 242 resonances in the n + ^{232}Th reaction with neutron energies in the range $0 - 4$ keV. The results are once again very consistent among the different measures as indicated in Table II. The estimated value of D_0 is $16.1^{+0.6}_{-0.5}$ eV and is in very good agreement with the value 16.5 ± 0.4 eV from Ref. [36] and with Mughabghab's value of 15.82 ± 0.55 eV [16].

TABLE II: Estimates of f and D for 242 s-wave resonances with energies E_n in the range $0 - 4$ keV in the n + ^{232}Th system.

	Statistic					Overall
	NNSD	Δ_3	U	$\hat{Q}$	ρ	Result
f	0.98 ± 0.05	0.98 ± 0.01	$0.97^{+0.02}_{-0.01}$	$0.99^{+0.02}_{-0.03}$	0.95 ± 0.08	0.98 ± 0.01
D_0 (eV)	$16.1^{+0.9}_{-1.1}$	16.1 ± 0.6	16.0 ± 0.6	16.2 ± 0.7	15.6 ± 1.4	16.1 ± 0.6

VII. SUMMARY AND CONCLUSIONS

The motivation for determining the fraction of missing levels in neutron resonances is clear and compelling – better values for the level density are crucial for a wide range of pure and applied nuclear science. The standard methods all assume the validity of the Gaussian Orthogonal Ensemble version of Random Matrix Theory, in particular that the Porter-Thomas distribution describes the width distribution. This approach often works very well, but non-statistical effects can lead to incorrect results. Since the very existence of such effects is essentially impossible to predict and very difficult to characterize and correct for in practice, other methods seem highly desired.

The key to alternate methods is that in RMT the widths and spacings are independent of one another. Since the spacing distribution is not affected by non-statistical effects while the width distribution can be strongly affected, this provides even more motivation. Even if analysis methods based on the width and spacing distributions agree, this adds to confidence in the results, as well as reducing the uncertainty in the value of the missing level correction.

Our initial focus was on the nearest neighbor spacing distribution [20]. In this case the levels were missed at random, complicating the analysis relative to the width analysis where the majority of missing levels were the weakest. In addition, once levels are missed, then one is actually studying the distribution of second-nearest neighbors, third-nearest, etc. This combination of difficulties is presumably the primary reason that this method had never been seriously pursued.

There are a variety of other measures that are used to evaluate whether spectra agree with RMT predictions. The Dyson-Mehta Δ_3 statistic is the most commonly used of these measures. Mulhall *et al.* [32] first applied this to the missing level problem. Dyson originally used the thermodynamics in order to address the missing level problem, but this approach was never used in practice until the present authors applied the thermodynamic energy as a test [31]. In the present work we also use another statistic first invented by Dyson and Mehta. As a final measure we considered the linear correlation coefficient for adjacent spacings. For all of these four measures, there is a specific prediction for the value of the statistic, either in the thermodynamic limit for large N, or for a specific value of N (in the case of Δ_3). Therefore given the experimental value of the statistic, there is a one-to-one correspondence with the value of the missing fraction f. As we see in the two applications examined here, these large variety of tests, which address different aspects of the spacing distribution, are in general in good agreement – especially when f is relatively large. One major drawback is that the effect of missing levels and of spurious levels are similar for all of the tests except for the nearest neighbor distribution. Thus, one needs to be fairly confident that spurious levels are minimal in any data set before relying on these techniques.

One example we presented was for the s-wave resonance set for ^{238}U. The observed level density D_0 is 22.3 eV for the energy range $0-20$ keV. Our value for the fraction of levels actually observed for this energy range is 0.85 ± 0.02. This leads to a corrected value of D_0 as 19.0 ± 0.6 eV. In general all of the tests are in agreement, although the fluctuations for some of the measures seem rather large. Applications of these newer tests to a variety of data sets will be valuable in order to establish the systematic behavior of the various measures for actual data. Lacking such a systematic study, and keeping in mind the fact of the possible effects of spurious levels, one might be tempted to accept the missing fraction determined from the nearest-neighbor spacing distribution. This gives an observed fraction $f = 0.88 \pm 0.03$ and corresponds to $D_0 = 19.6 \pm 0.8$ eV. It is interesting to note that this value agrees with that of Capote *et al.* [36] of $D_0 = 20.3 \pm 0.6$ eV. It is encouraging that our method using the spacings agrees well with the latest evaluation of ^{238}U s-wave resonances using the widths to make the correction. This is consistent with no non-statistical behavior in this energy region of ^{238}U. However, there are suggestions of spurious levels included in the s-wave date set. A second example for s-wave resonances in n + ^{232}Th was also discussed. For this example all of the tests were in excellent agreement, consistent with the ^{232}Th data set being essentially perfect.

Acknowledgments

This work was supported in part by the US Department of Energy under grants DE-FG02-97ER41042 and DE-FG02-96ER40990 and the National Nuclear Security Agency under grant DE-FG52-09NA29460.

APPENDIX I

The fitting functions, coefficients, and error matrices for each statistic are summarized in Table III.

TABLE III: Summary of fits and error matrices for each statistic

Statistic	Fitting function	Coefficients	Error matrix
$\tilde{f}$	$\tilde{f}(f_m, N) = a_0 + a_1 f_m$	$a_0 = 0.993$ $a_1 = -0.972$	$\begin{pmatrix} 7.32\times10^{-5} & -2.03\times10^{-4} \\ -2.03\times10^{-4} & 1.66\times10^{-3} \end{pmatrix}$
Δ_3	$\Delta_3(f_m, N) = b_0 f_m \frac{N}{30} + b_1 (1-f_m)^2 \times \Delta_{3,GOE}\left(\frac{N}{2[1-f_m]}\right)$	$b_0 = 0.920$ $b_1 = 0.978$	$\begin{pmatrix} 6.64\times10^{-3} & -9.99\times10^{-4} \\ -9.99\times10^{-4} & 4.15\times10^{-3} \end{pmatrix}$
U	$U(f_m, N) = c_0 + (c_1 + c_2 N) f_m$	$c_0 = 0.363$ $c_1 = 0.848$ $c_2 = 0.00183$	$\begin{pmatrix} 1.62\times10^{-4} & -5.54\times10^{-4} & -1.74\times10^{-7} \\ -5.54\times10^{-4} & 2.03\times10^{-2} & -2.55\times10^{-5} \\ -1.74\times10^{-7} & -2.55\times10^{-5} & 8.12\times10^{-8} \end{pmatrix}$
$\hat{Q}$	$\hat{Q}(f_m, N) = d_0 + d_1 f_m$	$d_0 = 0.337$ $d_1 = 0.897$	$\begin{pmatrix} 1.17\times10^{-4} & -3.85\times10^{-4} \\ -3.85\times10^{-4} & 2.72\times10^{-3} \end{pmatrix}$
ρ	$\rho(f_m, N) = e_0 + e_1 f_m$	$e_0 = -0.251$ $e_1 = 0.428$	$\begin{pmatrix} 2.67\times10^{-4} & -7.44\times10^{-4} \\ -7.44\times10^{-4} & 3.22\times10^{-3} \end{pmatrix}$

APPENDIX II

Included in this appendix are graphs for s-wave resonances in the n + ^{283}U reaction with $E_n = 0-4$ keV; these are analogous to those shown in Sect. VI for the energy range $E_n = 0-20$ keV.

[1] T. Belgya, O. Bersillon, R. Capote, T. Fukahori, Z. Ge, S. Goriely, M. Herman, A. Ignatyuk, S. Kailas, A. Koning, et al., Tech. Rep. IAEA-TECDOC-1506, International Atomic Energy Agency, Vienna, Austria (2006), see *http://www-nds.iaea.org/RIPL-2*.
[2] L. M. Bollinger and G. E. Thomas, Phys. Rev. **171**, 1293 (1968).
[3] S. J. Lokitz, G. E. Mitchell, and J. F. Shriner Jr., Phys. Rev. C **71**, 064315 (2005).
[4] C. E. Porter, *Statistical Theories of Spectra* (Academic Press, New York, 1965).
[5] H. I. Liou, H. S. Camarda, S. Wynchank, M. Slagowitz, G. Hacken, F. Rahn, and J. Rainwater, Phys. Rev. C **5**, 974 (1972).
[6] H. I. Liou, H. S. Camarda, and F. Rahn, Phys. Rev. C **5**, 1002 (1972).
[7] O. Bohigas, R. U. Haq, and A. Pandey, in *Nuclear Data for Science and Technology*, edited by K. H. Bockhoff (Kluwer Academic Publishing, Brussels, 1983), p. 809.
[8] E. G. Bilpuch, A. M. Lane, J. D. Moses, and G. E. Mitchell, Phys. Rep. **28**, 145 (1976).
[9] T. A. Brody, J. Flores, J. B. French, P. A. Mello, A. Pandey, and S. S. M. Wong, Rev. Mod. Phys. **53**, 385 (1981).
[10] T. Guhr, A. Müller-Groeling, and H. A. Weidenmüller, Phys. Rep. **299**, 189 (1998).
[11] H. A. Weidenmüller and G. E. Mitchell, Rev. Mod. Phys. **81**, 539 (2009).
[12] C. E. Porter and R. G. Thomas, Phys. Rev. **104**, 483 (1956).
[13] F. Fröhner, in *Nuclear Theory for Applications* (IAEA, Vienna, 1980), vol. IAEA-SMR-43, p. 59.
[14] M. S. Moore, J. D. Moses, G. A. Keyworth, J. W. T. Dabbs, and N. W. Hill, Phys. Rev. C **18**, 1328 (1978).
[15] Y. V. Porodzinskij, E. S. Sukhovitskij, and V. M. Maslov, Tech. Rep. INDC(BLR)-012, IAEA, Vienna (1998).
[16] S. F. Mughabghab, *Atlas of Neutron Resonances* (Academic Press, New York, 2006).
[17] P. E. Koehler, J. L. Ullmann, T. A. Bredeweg, J. M. O'Donnell, R. Reifarth, R. S. Rundberg, D. J. Vieira, and J. M. Wouters, Phys. Rev. C **76**, 02584 (2007).
[18] S. Åberg, A. Heine, G. E. Mitchell, and A. Richter, Phys. Lett. B **598**, 42 (2004).
[19] W. A. Watson, III, E. G. Bilpuch, and G. E. Mitchell, Nucl. Instr. Meth. **188**, 571 (1981).

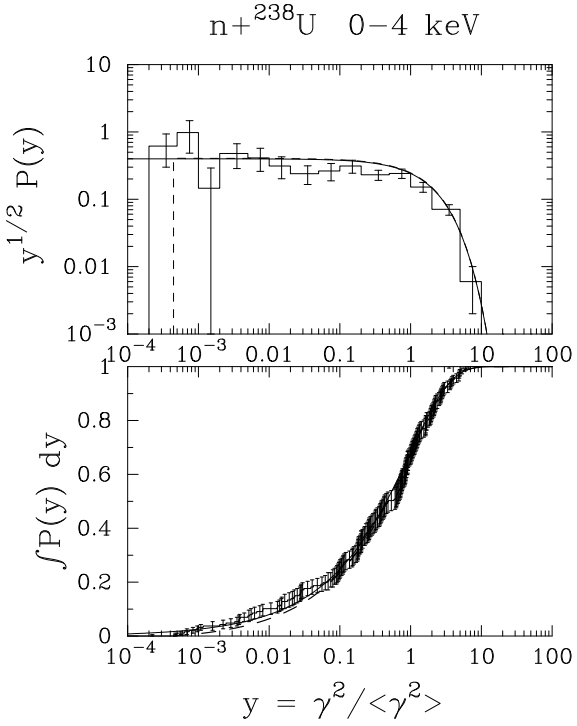

(a) Distribution of reduced widths. The histogram (upper) and the probability distribution function (lower) are shown.

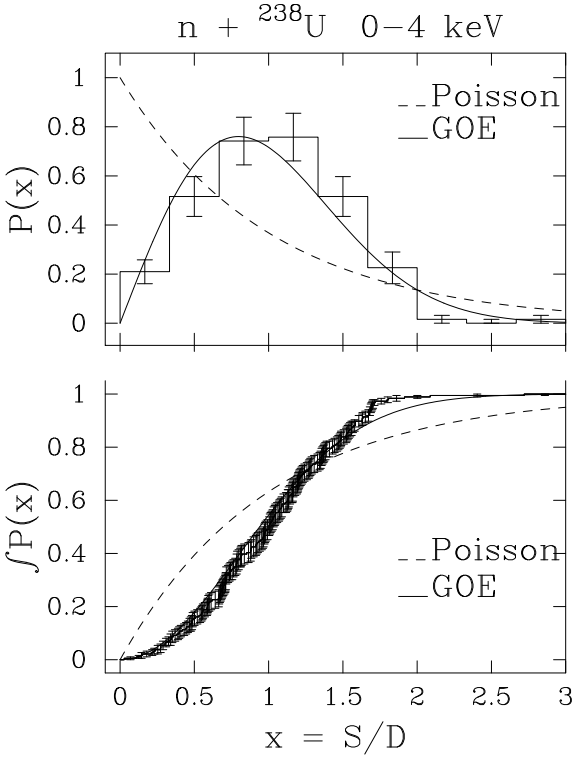

(b) Nearest-neighbor spacing distribution. The upper part of the figure shows the probability density function, while the lower portion shows the probability distribution function.

FIG. 6: Analysis of s-wave resonances in the n + ^{238}U reaction in the neutron energy range $0 - 4$ keV.

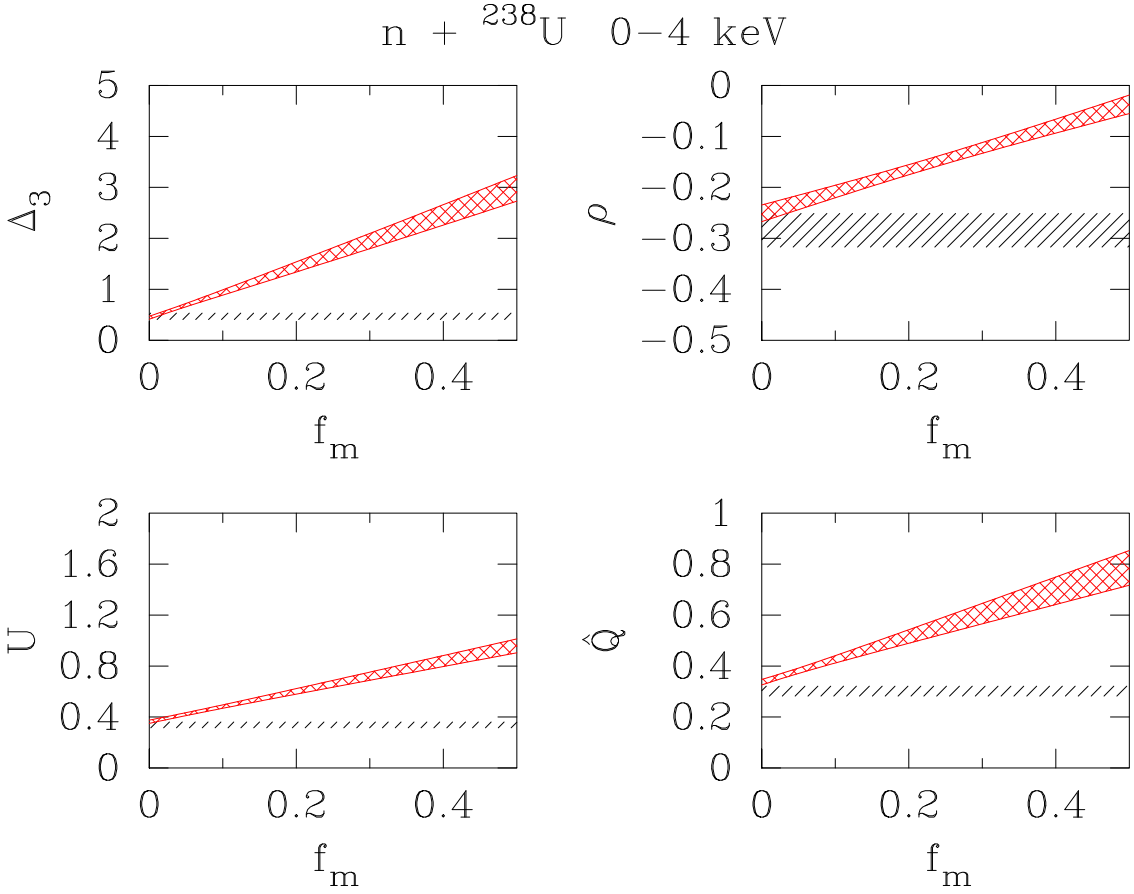

FIG. 7: Analysis of Δ_3, U, $\hat{Q}$ and ρ for the s-wave resonances with $E_n = 0-4$ keV in the n + ^{238}U reaction. The black dashed horizontal bands in each case represent the value of that statistic (± one standard deviation), and the red crossed bands show the expected behavior (again, ± one standard deviation) as a function of f_m for $N = 897$.

[20] U. Agvaanluvsan, G. E. Mitchell, J. F. Shriner, Jr., and M. Pato, Nucl. Instr. Meth. **A498**, 459 (2003).
[21] O. Bohigas and M. P. Pato, Phys. Lett. B **595**, 171 (2004).
[22] M. L. Mehta, *Random Matrices* (Academic, New York, 1991), 2nd ed.
[23] W. H. Press, S. A. Teukolsky, W. T. Vetterling, and B. P. Flattery, *Numerical Recipes in Fortran 77: The Art of Scientific Computing* (Cambridge University Press, New York, 1992), 2nd ed.
[24] J. B. French, P. A. Mello, and A. Pandey, Ann. Phys. (NY) **113**, 277 (1978).
[25] F. J. Dyson, J. Math. Phys. **3**, 140 (1962).
[26] F. J. Dyson, J. Math. Phys. **3**, 157 (1962).
[27] F. J. Dyson, J. Math. Phys. **3**, 166 (1962).
[28] F. J. Dyson and M. L. Mehta, J. Math. Phys. **4**, 701 (1963).
[29] M. L. Mehta and F. J. Dyson, J. Math. Phys. **4**, 713 (1963).
[30] O. Bohigas and M. J. Giannoni, Ann. Phys. (NY) **89**, 393 (1975).
[31] J. F. Shriner, Jr., M. P. Pato, G. E. Mitchell, and A. P. B. Tufaile, Nucl. Instr. Meth. **A581**, 831 (2007).
[32] D. Mulhall, Z. Huard, and V. Zelevinsky, Phys. Rev. C **76**, 064611 (2007).
[33] M. Chadwick, P. Obložinský, M. Herman, N. Greene, R. McKnight, D. Smith, P. Young, R. MacFarlane, G. Hale, S. Frankle, et al., Nucl. Data Sheets **107**, 2931 (2006).
[34] International Network of Nuclear Reaction Data Centres: EXFOR/CSISRS database, available online at http://www-nds.iaea.org/exfor/.
[35] J. E. Lynn, *The Theory of Neutron Resonances* (Clarendon, Oxford, 1968).
[36] R. Capote, M. Herman, P. Obložinský, P. Young, S. Goriely, A. I. T. Belgya and, A. Koning, S. Hilaire, V. Plujko, M. Avrigeanu, et al., Nucl. Data Sheets **110**, 3107-3214 (2009).

Nuclear Data Section
International Atomic Energy Agency
P.O. Box 100
A-1400 Vienna
Austria

e-mail: services@iaeand.iaea.org
fax: (43-1) 26007
telephone: (43-1) 2600-21710
Web: http://www-nds.iaea.org